Atherosclerosis Progression and Fractional Flow Reserve in Coronary Arteries

Filipovic, Nenad; Nikolic, Dalibor; Saveljic, Igor; Milosevic, Zarko; Isailovic, Velibor; Nikolic, Milica; Cirkovic-Andjelkovic, Bojana; Vukicevic, Arso; Jagic, Nikola; Themis, Exarchos; Fotiadis, Dimitris; Pelosi, Gualtiero; and Parodi, Oberdan

Abstract: ***In this study Fractional Flow Reserve (FFR) was compared to real clinical data from a specific patient. Also, plaque progression model was included. The Navier-Stokes and continuity equations were used for blood flow and pressure distribution for FFR. The system of three additional reaction-diffusion equations that models the inflammatory process and lesion growth model in the intima was used. The measured FFR threshold was 0.84 and computational 0.87. We found a good correlation between real and computed FFR results of the patient. Some examples of plaque formation and progression for the specific patient for left coronary artery are presented. Determination of virtual FFR and plaque progression with computer simulation for the specific patient shows a potential benefit for risk prediction of disease progression.***

Index Terms: ***coronary arteries, FFR simulation; plaque development***

1. INTRODUCTION

Fractional flow reserve (FFR) is an index of the hemodynamic significance of a coronary lesion. It is defined as the ratio of maximum flow in the presence of stenosis to normal maximum flow. It can be calculated by simultaneous measurement of mean arterial, distal coronary, and central venous pressure. There is very well known clinical evidence that FFR-guided percutaneous coronary intervention is associated with better clinical outcomes and reduces the need for repeated revascularisation. But, there are still limited clinical applications in everyday practice, mainly because it is a relatively expensive and time-consuming procedure [1]. To overcome these limitations, computational-based methodologies enable the estimation of FFR in three-dimensional models derived from anatomic imaging data.

Quantitative coronary angiography (QCA) has been the traditional method for estimating the extent and severity of coronary artery disease. However, cumulative evidence has shown that it has a modest accuracy in assessing the hemodynamic significance of intermediate lesions [2].

Atherosclerosis is a progressive disease characterized in particular by the accumulation of lipids and fibrous elements in artery walls. During the past decade, scientists came to appreciate a prominent role of inflammation in atherosclerosis. Atherosclerosis is characterized by dysfunction of endothelium, vasculitis and accumulation of lipid, cholesterol and cell elements inside blood vessel wall. This process develops in arterial walls [3]. Atherosclerosis develops from oxidized low-density lipoprotein molecules (LDL). When oxidized LDL evolves in plaque formations within an artery wall, a series of reactions occur to repair the damage to the artery wall caused by oxidized LDL [4]. Inflammatory process starts with penetration of low density lipoproteins (LDL) in the intima.

Several mathematical models have described the transport of macromolecules, such as low-density lipoproteins, from the arterial lumen to the arterial wall and inside the wall [5,6]. It is now well known that the early stage of the inflammatory disease is the result of interaction between plasma low density lipoproteins that filtrate through endothelium into the intima, cellular components (monocytes/macrophages, endothelial cells and smooth muscle cells) and the extracellular matrix of the arterial wall.

Manuscript received June 30, 2017. This work was supported in part by the grants III41007 and OI 174028 from the Ministry of Science, Education and Technological Development in Serbia, and grants HORIZON2020 689068 SMARTOOL and SCOPES JRP/IP IZ73Z0_152454.

N. Filipovic, D. Nikolic, Z. Milosevic, I. Saveljic, V. Isailovic, M. Nikolic, B. Andjelkovic-Ciric and A. Vukicevic are with the BioIRC, Bioengineering Research and Development Center, 6 Prvoslava Stojanovica Street, 34000 Kragujevac, Serbia (e-mail: fica@kg.ac.rs) and with the Faculty of Engineering, University of Kragujevac, 6 Sestre Janjic Street, 34000 Kragujevac, Serbia (e-mail: markovac85@kg.ac.rs).

N. Jagic is with Clinical Center Kragujevac, Kragujevac, Serbia, (e-mail: njagic@yahoo.com).

T.Exarchos and D. Fotiadis are with the University of Ioannina, Department for Material Science, Ioannina, Greece (e-mail: themis.exarchos@gmail.com).

G. Pelosi and O. Parodi are with the National Research Council Pisa, Pisa, Italy, (e-mail: oberdan.parodi@virgilio.it).

Our approach for simulation of the plaque formation starts with mass transport of LDL through the wall and the simplified inflammatory process which is coupled with the Navier-Stokes equations, the Darcy equation for model blood filtration and Kedem-Katchalsky equations [7,8] for the solute and flux exchanges between the lumen and the intima. We used three additional reaction-diffusion equations for the inflammatory process and lesion growth model in the intima. The specific patient left coronary artery plaque concentration (position and concentration) for CTA follow up is presented. FFR was calculated as steady state solution with pressure distribution for total anatomical tree. We firstly presented methodology section with continuum approach for FFR calculation and plaque progression. Then, certain results for FFR and plaque progression are given. Finally, some discussion and conclusions are described.

2. METHODS

We firstly described mass transfer problem for LDL transport through the wall and then a continuum based approach for plaque formation and development in three-dimension is described. The governing equations and numerical procedures are given. The blood flow in lumen domain is simulated by the three-dimensional Navier-Stokes equations, together with the continuity equation

$$\frac{\partial u_l}{\partial t} - \mu \nabla^2 u_l + \rho \left(u_l \cdot \nabla \right) u_l + \nabla p_l = 0 \tag{1}$$

$$\nabla u_l = 0 \tag{2}$$

where $\boldsymbol{u_l}$ is blood velocity in the lumen, p_l is the pressure, μ is the dynamic viscosity of the blood, and ρ is the density of the blood [9].

Mass transfer in the blood lumen is coupled with the blood flow and modeled by the convection-diffusion equation as follows:

$$\frac{\partial c_l}{\partial t} + \nabla \cdot \left(-D_l \nabla c_l + c_l u_l \right) = 0 \tag{3}$$

in the fluid domain, where c_l is the solute concentration in the blood lumen, and D_l is the solute diffusivity in the lumen.

Mass transfer in the arterial wall is coupled with the transmural flow and modeled by the convection-diffusion-reaction equation as follows

$$\frac{\partial c_w}{\partial t} + \nabla \cdot \left(-D_w \nabla c_w + k u_w c_w \right) = r_w c_w \tag{4}$$

in the wall domain, where c_w is the solute concentration in the arterial wall, D_w is the solute diffusivity in the arterial wall, K is the solute lag coefficient, and r_w is the consumption rate constant.

LDL transport in the vessel lumen is coupled with Kedem-Katchalsky equations:

$$J_v = L_p \left(\Delta p - \sigma_d \Delta \pi \right) \tag{4}$$

$$J_s = P \Delta c + \left(1 - \sigma_f \right) J_v \bar{c} \tag{5}$$

where L_p is the hydraulic conductivity of the endothelium, Δc is the solute concentration difference across the endothelium, Δp is the pressure drop across the endothelium, $\Delta \pi$ is the oncotic pressure difference across the endothelium, σ_d is the osmotic reflection coefficient, σ_f is the solvent reflection coefficient, P is the solute endothelial permeability, and $\bar{c}$ is the mean endothelial concentration.

The first term in Kedem-Katchalsky equations $P\ \Delta c$ of the right hand side in (Eq. 6) defines the diffusive flux across the endothelium, while the second term $\left(1 - \sigma_f \right) J_v \bar{c}$ defines the convective flux. Here we do not neglect the convective term. Only the oncotic pressure difference $\Delta\pi$ is neglected because of decoupling the fluid dynamics from solute dynamics. We used the incremental-iterative procedure to treat the convective diffusion terms for LDL transport.

The inflammatory process was solved using three additional reaction-diffusion partial differential equations [10]:

$$\begin{aligned} \partial_t Ox &= d_1 \Delta Ox - k_1 Ox \cdot M \\ \partial_t M + div(v_w M) &= d_2 \Delta M - k_1 Ox \cdot M + S/(1+S) \\ \partial_t S &= d_3 \Delta S - \lambda S + k_1 Ox \cdot M + \gamma (Ox - Ox^{thr}) \end{aligned} \tag{7}$$

where Ox is the oxidized LDL in the wall, M and S are concentrations in the intima of macrophages and cytokines, respectively; d_1, d_2, d_3 are the corresponding diffusion coefficients; λ and γ are degradation and LDL oxidized detection coefficients; and v_w is the inflammatory velocity of plaque growth, which satisfies Darcy's law and continuity equation [11]:

$$v_w - \nabla \cdot \left(p_w \right) = 0 \tag{8}$$

$$\nabla v_w = 0 \tag{9}$$

Shear stress distribution was calculated with standard tangential velocity derivative [12]. FFR calculation was calculated with standard Navier-Stokes and continuity equation with steady state flow and specific boundary conditions.

3. RESULTS

Three-dimensional reconstruction from a specific patient data was done from CT. Typical angiography image from this patient has been presented in Figure 1. The special guide wire crosses the lesion and is able to measure the flow and pressure of the blood, after infusion of a hyperemic agent, such as adenosine. Results are displayed on a special monitor with the value 0.84 which corresponds to inducible ischemia, and most likely will require interventional treatment.

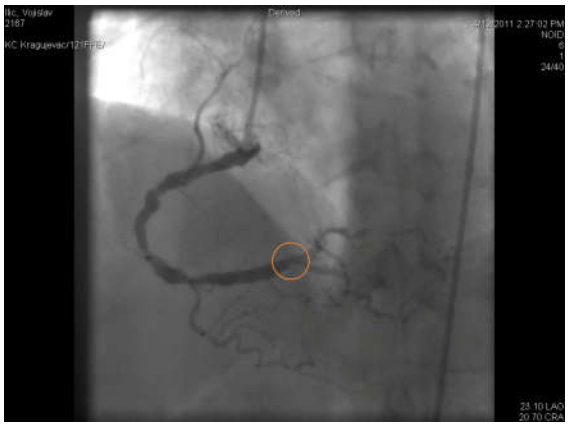

Fig. 1. Angiography image from patient

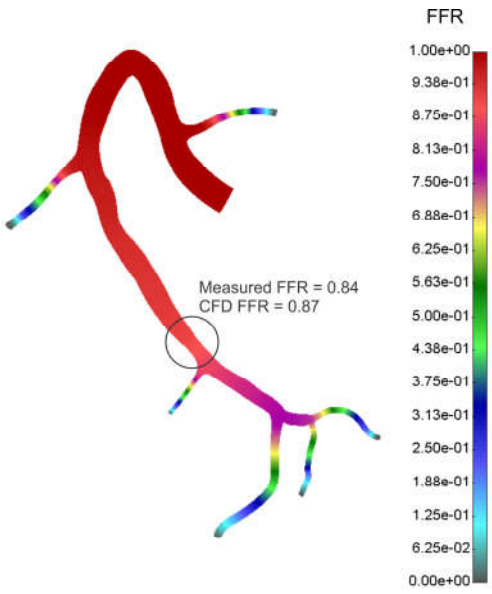

Fig. 2. FFR distribution

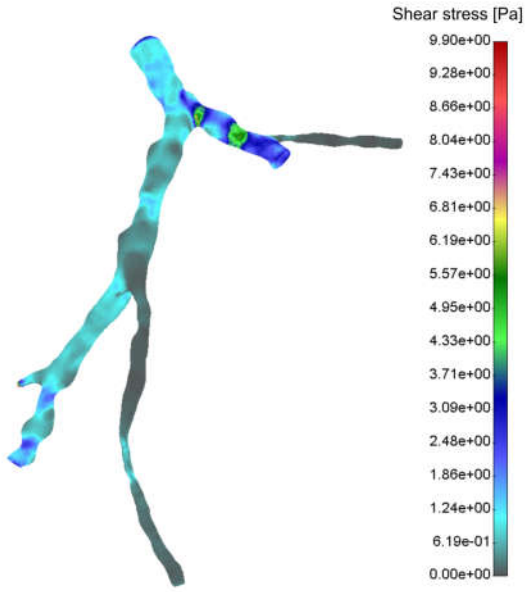

Fig. 3. Shear stress distribution

Computational FFR distribution for this patient was presented in Figure 2. The comparison with real clinical measurement of FFR (0.84) and computer simulation CFD (0.87) has been also presented. It can be observed that good accuracy was achieved.

Plaque progression for the patient at left coronary artery was detected using CT image analysis at baseline and after 12 months. Volume progression from 50% to 70% was observed with segmentation and registration of CT images. Shear stress distribution was firstly examined. Downstream the bifurcation level with the second marginal branch, predominantly low WSS values occur at baseline (Figure 3). Location of the lowest WSS in the distal portion of the vessel corresponded to the site of plaque growth after 12 months. The biomolecular parameters Cholesterol, LDL, HDL and Triglycerides for the patient at baseline have been listed in Table 1. These parameters are used for the computer simulation. The maximal plaque concentrations are denoted with red color in Figure 4 which directly gives plaque volume for the left specific patient coronary artery.

Table 1. Biomolecular parameters for the specific patient at baseline

Time	Total Chole sterol	LDL	HDL	Triglycerides
Baseline	199	110	38	334

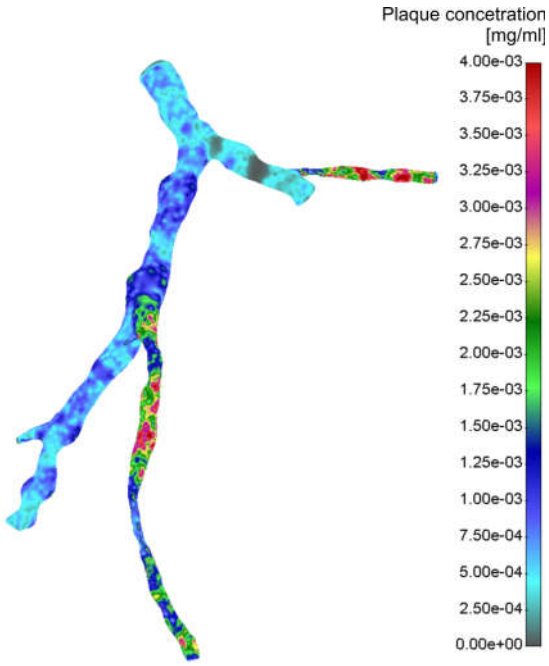

Fig. 4. Left coronary artery for the specific patient. Plaque concentration distribution.

4. CONCLUSION

We presented computational results for FFR and full three-dimensional model for plaque formation and development. Our modeling approach starts from partial differential equations with space and time variables and it describes the biomolecular process that takes place in the intima during the initiation and the progression of the plaque. The Navier-Stokes equations described the blood motion in the lumen, the Darcy law was used for model blood filtration, Kedem-Katchalsky equations for the solute and flux exchanges between the lumen and the intima. Additional reaction-diffusion equations were used for simulation of the inflammatory process and lesion growth model. Good matching between FFR measurements and simulation results were observed. Computer simulations data for the specific patient left coronary artery for plaque position and volume are presented. In silico modeling could be used for future diagnostic system for risk prediction of plaque development and FFR distribution.

REFERENCES

[1] Godoy G. K, Vavere A, Miller J. M, Chahal H, Niinuma H, Lemos P, Hoe J, Paul N, Clouse M. E, Ramos C. D, Lima J. A, Arbab-Zadeh A. Quantitative coronary arterial stenosis assessment by multidetector CT and invasive coronary angiography for identifying patients with myocardial perfusion abnormalities. *J Nucl Cardiol.*,2012, 19, pp. 922-930.

[2] Arnese M, Salustri A, Fioretti P. M, Cornel JH, Boersma E, Reijs A. E, De Feyter P. J, Roelandt J. R. Quantitative angiographic measurements of isolated left anterior descending coronary artery stenosis. Correlation with exercise echocardiography and technetium-99m 2-methoxy isobutyl isonitrile single-photon emission computed tomography. *J Am Coll Cardiol.* 1995, 25, pp. 1486-91.

[3] Loscalzo J, Schafer A. I, Thrombosis and Hemorrhage. Third edition. *Lippincott Williams & Wilkins, Philadelphia,* 2003.

[4] Begent N, Born G. V, 1970, *Nature*, 227, pp. 926–930.

[5] Tarbell JM, Mass transport in arteries and the localization of atherosclerosis. *Annual Review of Biomedical Engineering*, 2003, 5, pp. 79–118.

[6] Prosi M, Zunino P, Perktold K, Quarteroni A. Mathematical and numerical models for transfer of low-density lipoproteins through the arterial walls: a new methodology for the model set up with applications to the study of disturbed luminal flow. *J. Biomech.*, 2005, 38, 903–917.

[7] Kedem O, Katchalsky A. Thermodynamic analysis of the permeability of biological membranes to non-electrolytes. Biochim. *Biophys.* 1958, 27, pp. 229–246.

[8] Kedem O, Katchalsky A. A physical interpretation of the phenomenological coefficients of membrane permeability. *The Journal of General Physiology*, 1961, 45, pp. 143–179.

[9] Kojic M, Filipovic N, Stojanovic B, Kojic N, Computer Modeling in Bioengineering: Theoretical Background, Examples and Software. *John Wiley and Sons,* Chichester, England, 2008.

[10] Filipovic N, Zhongzhao T, Radovic M, Saveljic I, Fotiadis D. and Parodi O. Computer simulation of three dimensional plaque formation and progression in the carotid artery, *Medical & Biological Engineering & Computing,* 2013, DOI: 10.1007/s11517-012-1031-4.

[11] Filipovic N, Rosic M, Tanaskovic I, Milosevic Z, Nikolic D, Zdravkovic N, Peulic A, Fotiadis D, Parodi O. ARTreat project: Three-dimensional Numerical Simulation of Plaque Formation and Development in the Arteries, *IEEE Trans Inf Technol Biomed,* 2012, 16(2), pp. 272-278.

[12] Taylor C. A, Hughes T.J..R, Zarins C. K, Finite element modeling of blood flow in arteries, *Comp Meth Appl Mech Eng*, 1998, 158, pp. 155-196.